Cellulose (2010) 17:1159–1169
DOI 10.1007/s10570-010-9450-6

Microfiltration performance of regenerated cellulose membrane prepared at low temperature for wastewater treatment

Shilin Liu · Jian Zeng · Dandan Tao · Lina Zhang

Received: 31 May 2010 / Accepted: 1 September 2010 / Published online: 18 September 2010

Abstract A series of regenerated cellulose membranes with pore diameters ranging from 21 to 52 nm have been prepared by dissolving cellulose in 5 wt% LiOH/12 wt% urea aqueous solution re-cooled to −12 °C. The influences of cellulose concentration on the structure, pore size, and the mechanical properties of the membrane were studied by using Wide angle X-ray diffraction, scanning electron micrography and tensile testing. Their pore size, water permeability, equilibrium-swelling ratio and fouling behaviors of the cellulose membranes were characterized. The water-soluble synthetic and natural polymers as organic matter were used to evaluate the microfiltration performance of the regenerated cellulose membrane for wastewater treatment in aqueous system. The results revealed that the organic matter with molecular weight more than 20 kDa effected significantly on the membrane pore density, and reducing factor a_2, whereas that having molecular weight less than 20 kDa exhibited a little influence on the membrane pore size reducing factor a_1. Furthermore, a simple model to illustrate of microfiltration process of the RC membrane for wastewater treatment was proposed.

Keywords Cellulose membrane · Water permeability · Microfiltration · Pore size · Wastewater treatment

List of symbols

a_1	Membrane pore size change coefficient (m^{-1})
a_2	Pore density change coefficient (m^{-1})
d	Thickness of wet membrane (cm)
J_0	Permeability of the pure water (m^3/m^2 s)
J_{vi}	Flux of polluted water per unit membrane area (m^3/m^2 s)
N_i	Total number of pores per unit area (-)
P	Pressure (Pa)
P_r	Porosity of the wet membrane (%)
Q	Equilibrium-swelling ratio (-)
q_i	The accumulated permeate volume (m^3)
R	Pore diameter (cm)
r	The radius of the wet membrane (cm)
R_i	The mean pore diameter (cm)
RC	Regenerated cellulose
S_c	The area of all diffraction peaks of crystalline
S_a	The area of all diffraction peaks of amorphous
UFR	Ultrafilter rate of membrane for pure water (mL h^{-1} m^{-2} mm Hg^{-1})
W	Weight of the membrane at dry state (g)

S. Liu · J. Zeng · L. Zhang (✉)
Department of Chemistry, Wuhan University, 430072 Wuhan, China
e-mail: lnzhang@public.wh.hb.cn; linazhangwhu@gmail.com

S. Liu · D. Tao
College of Chemical and Material Engineering, Jiangnan University, 214122 Wuxi, Jiangsu, China

ρ_c Density of bulk cellulose (g cm^{-3})
ρ_m Density of the wet membrane containing pore (g cm^{-3})
σ_b Tensile strength (MPa)
ε_b Breaking elongation (%)
η The solvent viscosity (N s/m^2)
δ The length of the pores (μm)

Introduction

Since the development of asymmetric membrane by Loeb and Sourirajan (Loeb and Sourirajan 1963), membrane science and technology have attracted much attentions on the topic of separation science. Especially in industrial processes, it is receiving increasing interest in water and wastewater treatments, as well as in water recycling (Parameshwaran et al. 2001; Khayet et al. 2004). Unfortunately, the separation performance is limited by membrane fouling, which causes a decline in permeate flux, leading to increasing pressure with time and increases in the costs of water treatment (Zhao et al. 2000; Clech et al. 2006). Membrane fouling is a very complex process, which is not only influenced by the filtration mode (Mosqueda-Jimenez et al. 2004), but by the hydrodynamic conditions (Hong and Elimelech 1997), such as crossflow velocity and applied pressure. Moreover, the feed water chemistry (pH, ionic strength and divalent cation concentration) and membrane characteristics (pore size, membrane charge, and roughness) play important roles in the permeating performance (Burns and Zydney 1999; Capar et al. 2006; Pujar and Zydney 1994; Mehta and Zydney 2006; Teixeira et al. 2005). The permeability depends on the interactions between the foulant and the membrane and between the foulant and the fouling layer. Effects of the individual component such as bacteria, yeast, proteins and colloids have been examined to identify the mechanisms involved, as well as the influence of operating parameters in microfiltration and ultrafiltration (Belfort et al. 1994; Chan and Chen 2004; Marshall et al. 1993; Fane and Fell 1987). Furthermore, established models have been used to fitting the flux decline during filtration (Duclos-Orsello et al. 2006). However, there are significant gaps in our knowledge about mixed components in the filtration processes, because most of these models are only based on the effects of feed water components on the pore size of the membrane. Little attention has been directly put on the influence of the structural parameters of the membranes (pore size and pore density) on their permeating performance.

Cellulose is one of the most abundant and renewable natural polymers with relatively low cost, good compatibility with biological compounds, remarkable hydrophilic properties as well as its solvent resistance (Samir et al. 2004; Kim and Yun 2006). Moreover, regenerated cellulose membranes have also been widely used in membrane separation technique such as dialysis, ultrafiltration, fractionation and purification of mixtures etc. Dissolution of cellulose in alkali aqueous systems have been attracted much attention (Egal et al. 2008; Cuissinat and Navard 2006; Sescousse and Budtova 2009; Gavillon and Budtova 2007). Recently, we have developed an aqueous solvent system for cellulose dissolution at low temperature, namely 7.0 wt% NaOH/12.0 wt% urea, 9.5 wt% NaOH/4.5 wt% thiourea and 5 wt% LiOH/12 wt% urea precooled to $-5 \sim -12$ °C, and they have been used to prepare cellulose membranes (Cai et al. 2007a, b, 2008; Lue et al. 2007; Ruan et al. 2004a; Liu and Zhang 2009; Qi et al. 2008). It is noted that LiOH/urea/water solution system has a more powerful ability to dissolve cellulose, and the pore size and the porosity of the cellulose membranes can be controlled by changing the concentration of the cellulose solution and the coagulation temperature (Liu and Zhang 2009). It is well known that in ultrafiltration or microfiltration, the transmission rate of solute is determined mainly by the relative size of the solute and the membrane pores. Therefore, the pore size, size distribution and the density of the membranes are the important parameters for the separation technology. To fit the separation process of the cellulose membrane used in wastewater treatment, we attempted to use water-soluble synthetic and natural polymers as organic matter to evaluate the microfiltration performance of the regenerated cellulose membrane in aqueous system. This work can provide some information to improve the separation materials and to extend the applications of cellulose.

Experimental sections

Materials

Cellulose (cotton linter pulp) used was provided by Hubei Chemical Fiber Group Ltd (Xiangfan, China). The cellulose sample was washed with distilled water for five times and dried in a vacuum oven at 70 °C before use. Its viscosity-average molecular weight (M_η) was determined by using an *Ubbelohde* viscometer in LiOH/urea aqueous solution at 25 ± 0.05 °C and calculated from the equation $[\eta] = 3.72 \times 10^{-2} M_w^{0.77}$ to be 13.6×10^4 (Cai et al. 2008). Analytical grade Polyethylene glycol (PEG) and dextran with different molecular weight were, respectively provided by Xilong Chemical Ltd (China) and Sigma (USA). Other chemical regents were purchased from China with analytical grade and used without further purification.

Preparation of regenerated cellulose membrane

About 200 g aqueous LiOH/urea solution (5.0 wt%/12.0 wt%) was precooled to −12 °C in a refrigerator, and then a desired amount of cellulose was added into the solution immediately, with stirring for 5 min to dissolve. The resultant cellulose solution was subjected to centrifugation at 8,000 rpm for 10 min at 10 °C to eliminate bubbles in the viscous solution. The viscous bubble-free solution was casted on a glass plate and the thickness of the membranes was controlled to be 0.25 mm, and then the glass plate was immersed into the coagulating bath containing 5 wt% H_2SO_4 to coagulate and regenerate for 5 min at 30 °C. The regenerated cellulose (RC) membranes were firstly washed with running water, then with deionized water, and finally air-dried at ambient temperature. The RC membranes prepared from the cellulose solution with concentration of 4, 4.5, 5 and 5.5 wt% were coded as RC-4, RC-4.5, RC-5 and RC-5.5.

Membranes characterization

Wide angle X-ray diffraction (WAXD) measurement was carried out on a WAXD diffractometer (D8-Advance, Bruker, USA) in symmetric reflection mode. The patterns with Cu Kα radiation (the weighted average λ is 0.15418 nm) at 40 kV and 30 mA were recorded in the 2θ range of 4 to 40°. Native and regenerated cellulose were ground into powders and dried in vacuum oven at 60 °C for 48 h before testing. The crystallinity χ_c (%) of the samples was estimated by (Rabek 1980):

$$\chi_c = \int_0^\infty S^2 I_c(s) ds \Big/ \int_0^\infty S^2 I(s) ds \quad (1)$$

where s is the magnitude of the reciprocal-lattice vector and is given by $s = (2\sin\theta)/\lambda$, θ is one-half the scattering angle. λ is the X-ray wavelength, $I(s)$ is the intensity of the coherent X-ray scattering from a specimen (both crystalline and amorphous), $I(c)$ is the intensity of coherent X-ray scattering from the crystalline region.

Fourier-transform infrared (FTIR) spectra of the natural and RC membranes were recorded with FT-IR spectrometer (model 1600, Perkin-Elmer Co. USA). The tested samples were prepared by the KBr-disk method. The morphologies of the RC membranes were characterized by using scanning electron micrographs (SEM, FEI QUANTA 200, PHILIP). The wet membranes were frozen in liquid nitrogen snapped immediately, and then freeze-dried. The free surface (the side in contact with the coagulant) and the back surface (the side in contact with the glass plate) of the membranes were sputtered with gold before observation.

The equilibrium-swelling ratio (Q) of the wet membranes was estimated as follows. A piece of the membrane was immersed in distilled water for 5 days until it reached the swelling-equilibrium state, and then removed from the storage solution. The water on its surface was wiped off, and the wet membrane was weighed. The weighed membrane was dried in a vacuum oven at 70 °C for about 48 h and reweighed. The equilibrium-swelling ratio (Q) can be obtained (Bell and Peppas 1996):

$$Q = \frac{W_h - W_d}{W_d} \quad (2)$$

where W_h is the equilibrium weight of the swollen sample and W_d is the weight of the dried sample. Five replicates were performed to obtain an average value of Q.

The porosity of the wet RC membrane (P_r) with specific area can be estimated by measuring its

thickness d (cm) at the wet state and weight W (g) at the dry state and calculated by (Yang and Zhang 1996):

$$P_r = 1 - \frac{W}{\rho_c \pi r^2 d} \tag{3}$$

where r is the radius of the wet membrane, and ρ_c is the density of bulk cellulose (1.5 g cm^{-3}).

The pure water permeability test of the wet membranes was carried out on a miniature microfiltration equipment at ambient temperature under 0.1 MPa. Circular membrane discs were set with a porous support and tightened by a rubber O-ring. The effective permeation area of each membrane was about 7.07 cm^2. Prior to testing, the pure water flux was measured to ensure that the membrane used was stable. The ultrafiltration rate (UFR) of the wet membrane for pure water was calculated by:

$$UFR = \frac{V}{StP} \tag{4}$$

where UFR is the pure water permeability (mL h^{-1} m^{-2} Hg^{-1}); V is the volume of permeated water, t the time (h); P the pressure (Pa), and S is the effective surface areas of the membrane (7.07 $cm^{2)}$. The pore sizes ($2r_f$) of the cellulose membranes were determined by the Hagen-Poiseuille law:

$$\upsilon = \frac{\Delta p d^2}{32 \mu d} \tag{5}$$

where υ is the fluid velocity of fluid, Δp is the pressure drop across a membrane with thickness of d, μ is the viscosity of the fluid.

The tensile strength (σ_b) and elongation at break (ε_b) of the membrane at the dry and wet states were measured on a universal tensile tester (CMT 6503, Shenzhen SANS Test machine Co. Ltd, China) according to ISO 527-2, 1993 (E) at a speed of 5 mm min^{-1}, The σ_b and ε_b values were the average results of five measurements.

Structure parameter model for membrane

According to the filtration processes of a membrane, the dissolved matters in feed water are divided into two categories. One is correlated to the dissolved matter with low molecular size in feed water, which may permeate or form an adsorption layer inside the pores of the membrane and thus reducing the membrane pore size. The other refers to matter with larger molecular size that may form clogging on the membrane surface and reduce the pore density. Therefore, the pollutants in feed water may change the pore density and pore size of the membrane during the permeating process, and they are the important parameters to reflect the membrane filtration characteristics. By using the Hagen-Poiseuille equation, solvent flux (J_{vi}) through the pores having diameter R_i can be expressed as (Singh et al. 1998):

$$J_{vi} = \frac{\pi \Delta p R_i^4}{128 \eta \delta} N_i \tag{6}$$

where η is the solvent viscosity, δ is the length of the pores; J_{vi} is flux of the feed water, N_i is the membrane pore density having diameter of R_i (the membrane pore diameter is a function of time during the permeating process, so i is for a given time step; $i = 1, 2, 3\ldots$).

According to the hypothesis, during the membrane filtration processes of the feed water, the values R_0 and N_0 of the original membrane may change with accumulated permeate water volume per unit membrane area (q_i) as (Wang and Wang 2006):

$$R_i = (1 - a_1 q_i) R_0 \tag{7}$$

$$N_i = (1 - a_2 q_i) N_0 \tag{8}$$

where a_1 is the mean pore size reducing factor, and a_2 is pore density reducing factor. So, the following equations can be deduced from Eqs. (6), (7), (8):

$$J_{vi} = \frac{pDP(1 - a_1 q_i)^4 R_0^4}{128 hd} (1 - a_2 q_i) N_0 \tag{9}$$

where J_{vi} is the accumulated flux of feed water per unit membrane area when the accumulated permeate volume per unit membrane area is q_i. Equation (9) is defined as the membrane structure parameter model, which reflects that membrane flux changes with the accumulated permeate water volume per unit membrane area, according to Eqs. (6), (9), the following formula can be deduced:

$$\frac{J_{vi}}{J_0} = (1 - a_2 q_i)(1 - a_1 q_i)^4 \tag{10}$$

A series of experimental values of J_{vi}/J_0 and accumulated permeate per unit membrane area q_i are combined with Eq. (10), then the optimal values of a_1 and a_2 can be calculated via computer simulation.

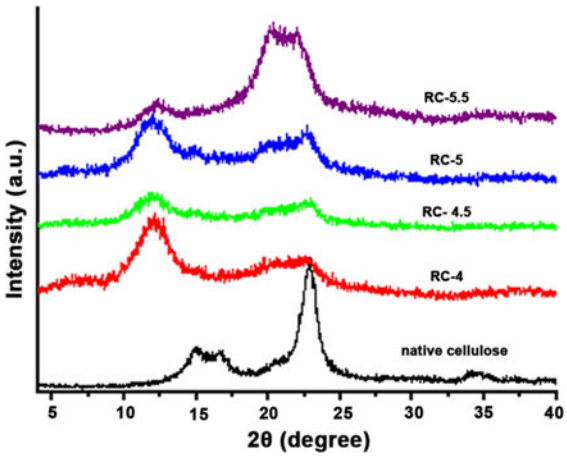

Fig. 1 WAXD patterns of the native cellulose and regenerated cellulose membranes

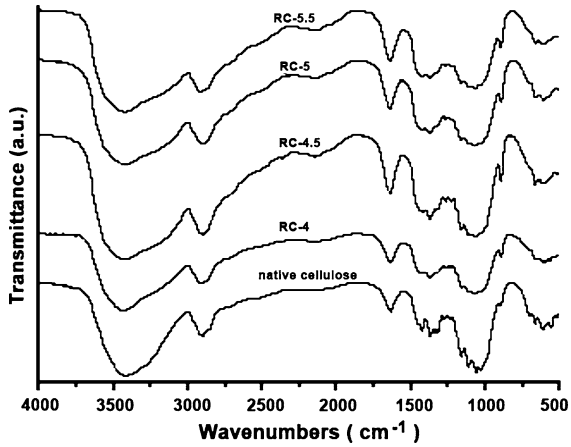

Fig. 2 FT-IR spectra of the native cellulose and the RC films prepared from different concentrations of cellulose

Results and discussion

Structure and pore size of the RC membranes

Figure 1 shows the WAXD patterns of the native cellulose sample and regenerated cellulose membranes. The crystalline form of native cellulose has typical diffraction peaks at $2\theta = 14.9$, 16.5 and 22.7°. The diffraction peaks at $2\theta = 12.2$, 20.2 and 21.6° of the RC membranes observed were assigned to the ($1\bar{1}0$), (110) and (200) planes of cellulose II crystal (Isogai et al. 1989). This indicated clearly that a conversion from cellulose I (native cellulose) to cellulose II (regenerated cellulose) occurred during dissolution and coagulation in the bath containing 5 wt% H_2SO_4. The values of χ_c (%) of the samples calculated from WAXD patterns are listed in Table 1. The χ_c (%) values of the RC membranes were lower than that of native cellulose, suggesting that the crystal structure of the native cellulose has been destroyed in the LiOH/urea solution, and a new crystal structure formed partly, leading to the predominance of non-crystalline regions. It was worth noting that the χ_c (%) value of the RC membrane (33.2%) prepared from 4 wt% cellulose solution was lower than that of the regenerated cellulose membranes prepared from NaOH/urea and NaOH/thiourea solution system with the same concentration (Zhou et al. 2002; Ruan et al. 2004b). It also suggested that LiOH/urea solution had a stronger ability to dissolve cellulose than NaOH/urea system by destroying the crystalline structure of the native cellulose.

FT-IR spectra of the native cellulose and RC membranes prepared from different concentration was shown in Fig. 2. The bands at 1,431 and 1,319 cm^{-1}, assigned to symmetric bending and wagging of $-CH_2$, respectively, shifted to lower wavenumbers in comparison with that of the native cellulose, indicating that a destruction of intermolecular hydrogen bonds involving the exocyclic hydroxyl groups (O_6) occurred. The band at 896 cm^{-1}, characteristic of the amorphous regions of cellulose, moved toward to lower wavenumbers. This further

Table 1 Experimental results of the regenerated cellulose membranes prepared with different concentrations of cellulose

Sample no	Cellulose concentration (%)	χ_c (%)	P_r (%)	$2r_f$ (nm)	*UFR* (mL h^{-1} m^{-2} mm Hg^{-1})
Native cellulose	–	72.6	–	–	–
RC-4	4.0	33.2	94.3	52.1	11.2
RC-4.5	4.5	33.9	92.9	46.3	10.8
RC-5	5.0	36.1	91.1	33.5	8.8
RC-5.5	5.5	41.2	90.1	21.2	8.4

provided an evidence for the transformation of the crystalline state from cellulose I to II (Sang et al. 2005). In comparison with native cellulose, the bands at 1,431 and 896 cm^{-1} for the RC membranes became weaker and stronger, respectively, indicating the decreased crystallinity of the regenerated cellulose. The results from FT-IR spectroscopy and X-ray diffraction demonstrated that a transition from cellulose I to cellulose II occurred during the membrane formation process.

Figure 3 shows the SEM micrographs of the free surface (the side directly in contact with the coagulant) and back surface (the side in contact with glass) of the RC membranes. All of the membranes displayed an asymmetric structure, namely, the pore size on the free surface was different from that on the back surface. With an increase of the cellulose concentration, the surface morphology of the membranes became denser, and the pore size (both the free and the back surfaces) decreased. The detail data of P_r, $2r_f$ and *UFR* of the RC membranes are summarized in Table 1. The RC-4 membrane had a distinct asymmetric structure including the free surface with many macrovoids and back surface with larger pores (Fig. 3a, e). However, when the concentration of cellulose was 4.5 wt%, the macroporous structure on the back surface and interpenetrated network structure on the free surface were formed, and the macrovoids became inconspicuous (Fig. 3b, f). In view of the results in Table 1, with an increase of the cellulose concentration from 4.0 to 5.5 wt%, the pore size ($2r_f$) of the cellulose membranes decreased from 52 to 21 nm. Therefore, by changing the cellulose concentration we can control the pore size of the RC membranes.

On the basis of the process of porous membrane formation (Kamide et al. 1993), the diffusion and convection between cellulose solution and coagulant play an important role in controlling the morphology and pore size of the membranes. In our findings, the cellulose was dissolved in LiOH/urea solvent to form clear liquid. When the cast sheet from the cellulose solution was immersed into coagulation bath, the diffusion between non-solvent and solvent in the casting cellulose solution (gel state) occurred. (Mao et al. 2006) With a large amount of non-solvent diffusion into the casting solution, the two-phase separation of cellulose rich-phase in the gel sheet and lean-phase in solution occurred, which was responsible for the formation of a porous structure. There was the mesh structure in the cellulose membranes (see Fig. 3), which was weaved with cellulose bunch in the cellulose rich-phase, as a result of the strong self-association force (Weng et al. 2004). In this process, cellulose backbone with semi-stiff molecular chain contributed to support the pore wall, whereas its –OH groups acted as formation of pore, because of its water absorbency. The penetration rate of the

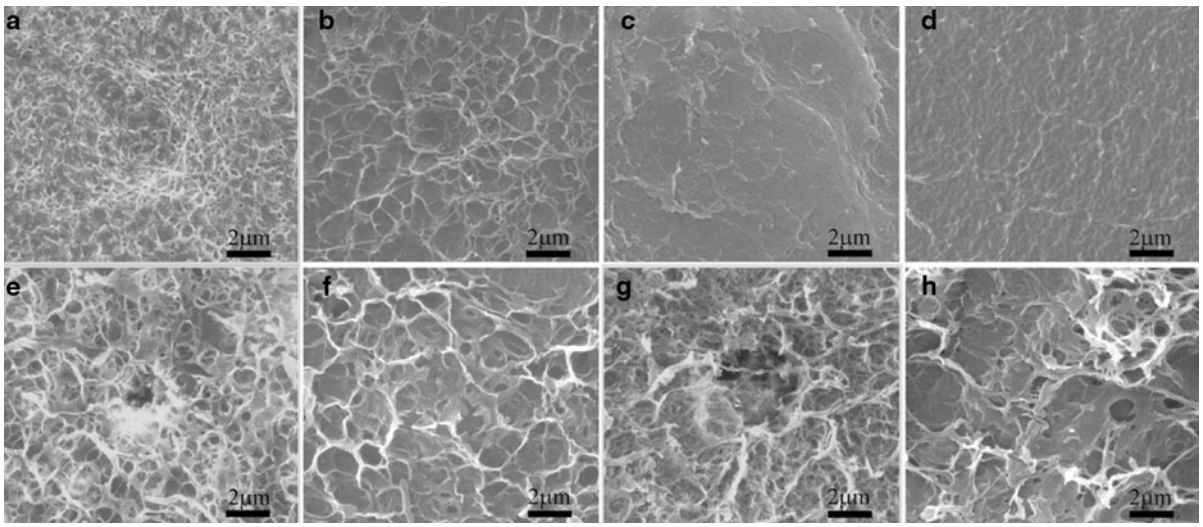

Fig. 3 SEM imagines of the back surface (**a**, **b**, **c**, **d**) and the free surface (**e**, **f**, **g**, **h**) of regenerated cellulose membranes prepared from different concentrations: 4% (**a**, **e**), 4.5% (**b**, **f**), 5% (**c**, **g**) and 5.5% (**d**, **h**), respectively

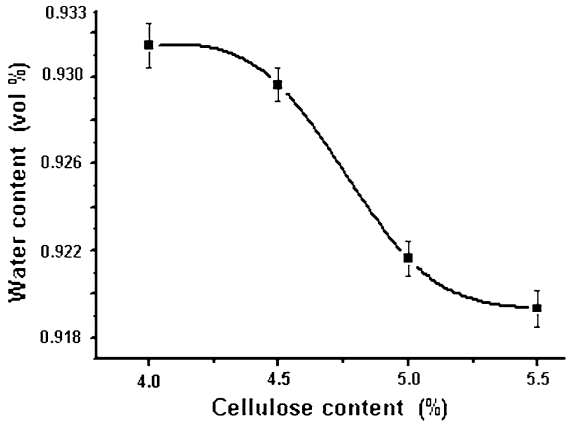

Fig. 4 Equilibrium-swelling degree (Q) of the regenerated cellulose membranes as a function of cellulose concentrations

coagulation bath on the free surface is faster than that of the back surface, resulting in an asymmetric structure. Moreover, with an increase in the cellulose concentration, the cellulose poor phase decreased, leading to the formation of a relatively denser structure and smaller pore size in the regenerated cellulose membranes.

Effects of pore size and density on the water flux

Figure 4 shows the equilibrium-swelling degree of the regenerated cellulose membranes as a function of cellulose concentration. With an increase of the cellulose concentration, the equilibrium-swelling ratios of the RC membranes decreased, further confirming that the pore size and density decreased. Therefore, there was a large resistance to matters passing through the membranes, leading to a decrease in the flux. The water permeability (*UFR*) decreased from 11.2 to 8.4 mL h^{-1} m^{-2} mm Hg^{-1}, when the concentration of the cellulose solution increased from 4 to 5.5 wt%. The results from *UFR* and water content of the membranes supported that the pore size decreased with an increase of the cellulose concentration.

The influences of the cellulose concentration on the tensile strength (σ_b) and elongation at break (ε_b) of the RC membranes at the dry and the wet state are shown in Fig. 5. The mechanical properties of the RC membranes prepared from the cellulose solution with concentration in the range of 4.0–5.5% changed hardly, and the mechanical properties of the RC membranes prepared from this LiOH/urea system

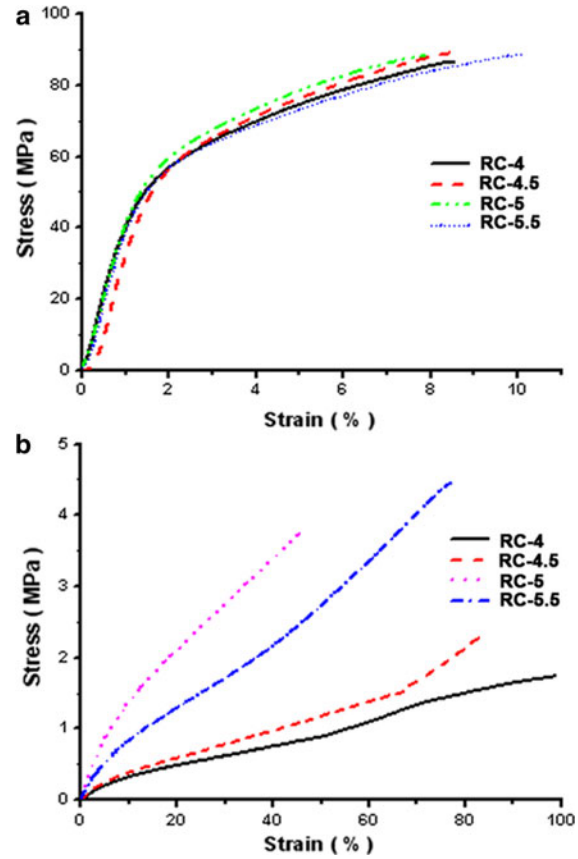

Fig. 5 The influence of cellulose concentration on the stress and strain of the RC films: **a** at dry state, **b** at wet state

was higher than those prepared from NaOH/urea and NaOH/thiourea solution system, as well as the commercial cellophane. Particularly, the RC membranes at the wet state exhibited good tensile strength, indicating that RC membrane can be used well at the wet state in water, and would have promising applications in the separation technology fields.

Effects of fouling on flux curves

The water-soluble PEG and dextran with different molecular weight as fouling source were added in the feed water. The apparent molecular weights of the organic matters were listed in Table 2. Figure 6 shows the flux curves of RC membranes with the accumulated permeate per unit membrane area. There was a sharp reduction in the flux at the beginning of the filtration process, which was an indicative of rather rapid reversible fouling taking place initially. The nearly constant permeate flux provided an

Table 2 The apparent molecular weight (M) and the content of organic matter in experimental feed water samples (mg/L)

Feed water sample	<4 kDa (mg/L)	4–10 kDa (mg/L)	10–20 kDa (mg/L)	20–40 kDa (mg/L)	>40 kDa (mg/L)
1#	173	36	15	12	13
2#	207	25	20	12	8
3#	213	17	11	6	10
4#	140	21	13	7	7
5#	196	23	15	6	5

indication of the formation of a surface fouling layer, probably resulting in a more compact and/or thicker layer, leading to the reduced flux. The fitted results from the established model were close to the experimental value, suggesting that the microfiltration membrane structure parameter model based on this study could be used to evaluate the microfiltration process of water. From the results in Table 2 and Fig. 6, the organic matters with molecular weight of 4–20 kDa played a key role on the control of the fouling of the RC membranes.

We calculated the molecular size and compared it to the pore size of the RC membrane according to the reported works (Tao et al. 2007), which was close to the minimum pore size of the cellulose membrane. Based on the results obtained in this work, the organic matter in different water-soluble samples could be divided into two categories: one with

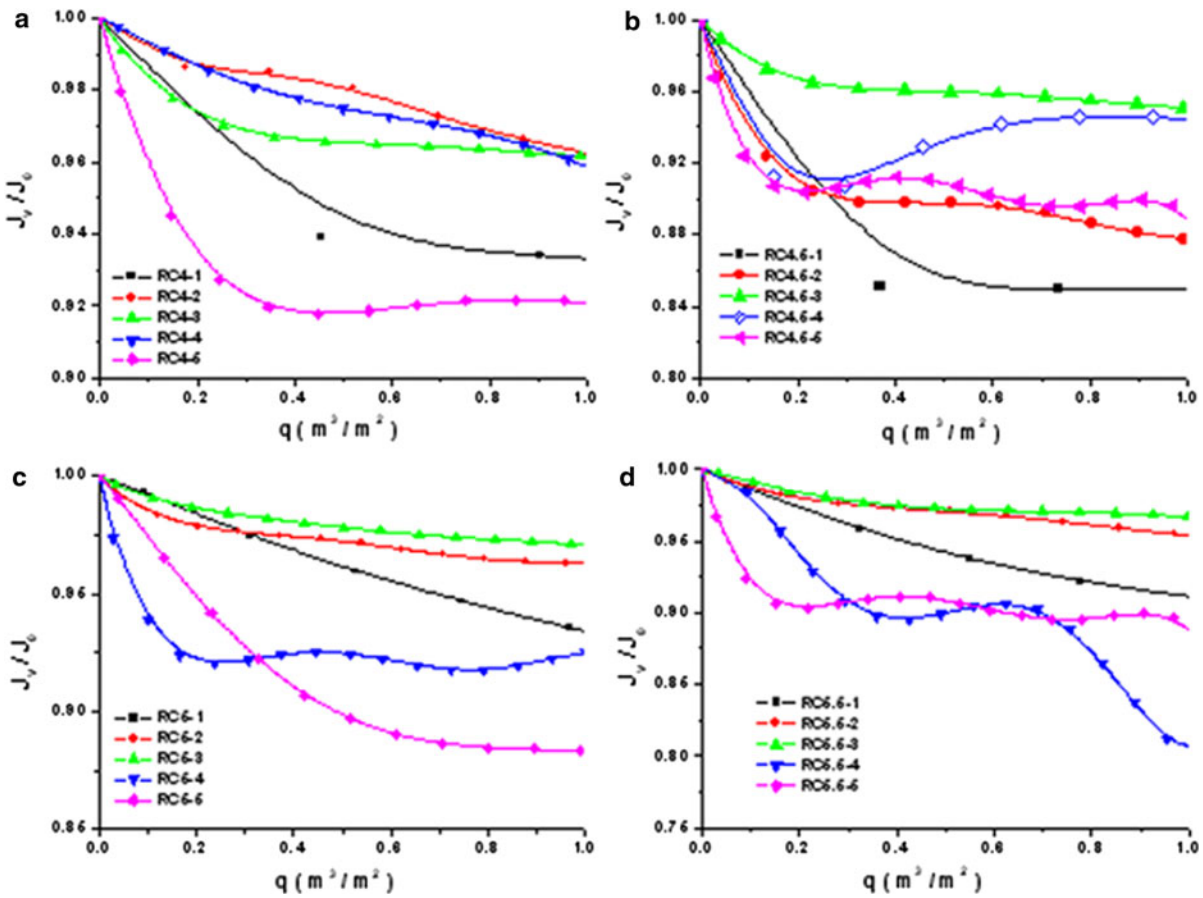

Fig. 6 Effects of the components of feed water on the fitted permeating performance of the RC membranes with different pore size and density

Table 3 The relationship between the fitting d values of model parameters (a_1 and a_2) of four RC membranes and five feed water samples with specified molecular weight (M)

Feed water sample			RC-4		RC-4.5		RC-5		RC-5.5	
No	Sample 2 M < 20 kDa (mg/L)	Sample 1 M > 20 kDa (mg/L)	a_1 (m^{-1})	a_2 (m^{-1})	a_1 (m^{-1})	a_2 (m^{-1})	a_1 (m^{-1})	a_2 (m^{-1})	a_1 (m^{-1})	a_2 (m^{-1})
1#	224	25	0.011	0.020	0.016	0.033	0.004	0.037	0.012	0.072
2#	252	20	0.004	0.017	0.026	0.031	0.007	0.040	0.004	0.067
3#	241	16	0.003	0.011	0.047	0.026	0.007	0.028	0.045	0.032
4#	174	14	0.013	0.010	0.030	0.019	0.030	0.022	0.007	0.030
5#	234	11	0.002	0.009	0.051	0.013	0.039	0.019	0.022	0.029

molecular weight larger than 20 kDa was coded as sample 1, and the other less than 20 kDa was coded as sample 2. Therefore, sample 2 in water could form adsorption layers inside the membrane pores to reduce the pore size, and sample 1 could form clogging in the membrane surface to decrease the pore density. The corresponding calculated values of a_1 (the membrane pore size change coefficient) and a_2 (the pore density change coefficient) in microfiltration process with water-soluble samples have been summarized in Table 3. The membrane pore density reducing factor a_2 decreased with an increase of the content of sample 1, and the trends of their changes for all the membranes were basically the same. This revealed that sample 1 mainly led to the reduction of the membrane pore density during the membrane filtration process. However, the trend of changes in a_1 from sample was different from that of a_2, it could be ascribed to the greater influence of sample 2 on a_1. When the wastewater had components with higher

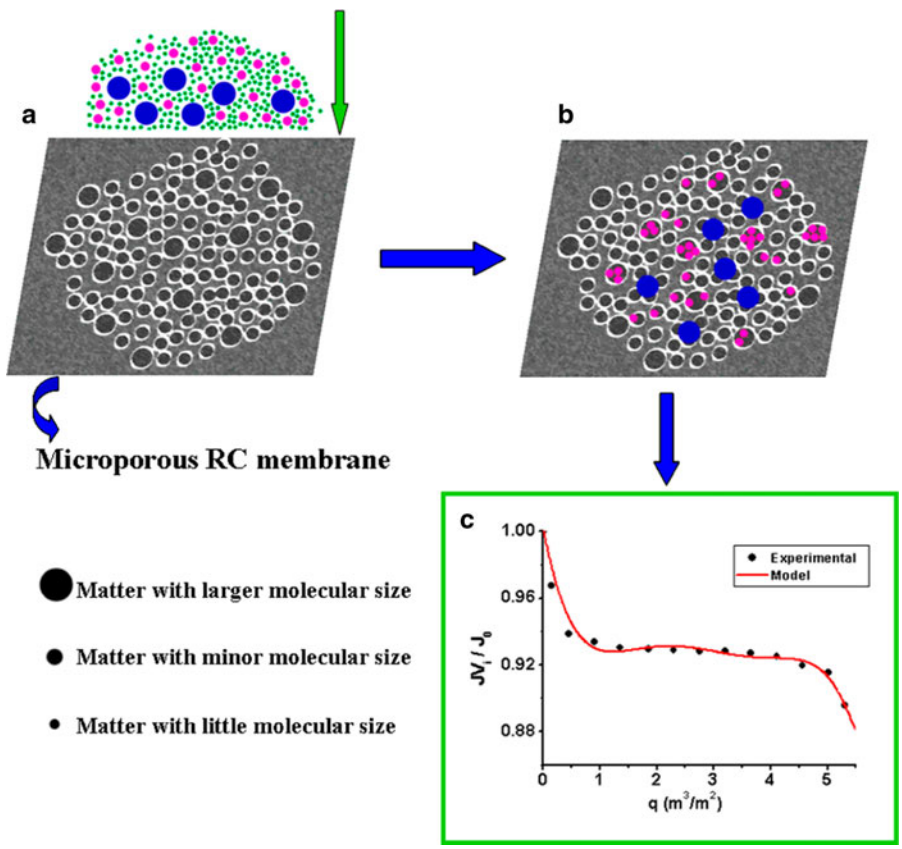

Fig. 7 Simplified illustration of microfiltration process of the RC membrane used for wastewater containing organics with different molecular size (**a**), (**b**), and fitted model curve and experimental result of RC-4 for microfiltration of wastewater sample 1 (**c**)

molecular weight, namely relatively larger hydrated radius (larger than the pore size of cellulose membrane). Therefore, it is difficult for them to penetrate through the cellulose membrane, and forms clogging on the surface or wall up the pores of the membrane to influence on a_2. However, a_1 was related to the components with lower molecular weight. The components with lower molecular weight in wastewater sometimes can be absorbed into the pores of the membrane, and they also can move into solution or penetrate through the membrane. The random values of a_1 would be resulted from the interaction of components with cellulose membrane; it was a dynamic process, leading to the complex process of separation process.

Modeling of the fouling behaviors

It has been reported that the salt concentration, ionic strength, Zeta potential, the hydrophilic and hydrophobic properties of organic matters, and as well as membrane parameters such as pore size, surface electric charge and the hydrophilic and hydrophobic properties, also affect the separation performance of the membrane (Yuan and Zydney 1999; Burns and Zydney 2000). In view of the above results, a schematic illustration for the microfiltration process of wastewater is proposed in Fig. 7. According to the pore size of the RC membrane, the organic matters in feed water with larger molecular size than the membrane pore size could form clogging on the membrane surface, leading to a decrease in the pore density of the membrane. However, the dissolved organic matters with molecular size smaller than the membrane pore size could penetrate the membrane or form adsorption layer inside the membrane to reduce membrane pore size. Therefore, the model used in our work could describe clearly the separation process. Appropriate pretreatment could then be adopted to achieve the purposes of reducing membrane fouling, which would promote flux efficiency and prolong the useful life of the membrane, as well as to lighten the environmental burden.

Conclusions

Regenerated cellulose membranes with different pore size have been successfully prepared from LiOH/urea solution system precooled to −12 °C. During coagulation, the two-phase separation of cellulose rich-phase in the gel sheet and lean-phase in solution occurred, which was responsible for the formation of a porous structure. The pore size of the regenerated cellulose membrane decreased with an increase of the cellulose concentration, resulting in a decline in permeability of the membrane. However, the mechanical properties of the membrane changed hardly by varying the concentration of cellulose. The water-soluble synthetic and natural polymers as organic matter were used to evaluate the microfiltration performance of the regenerated cellulose membrane in aqueous system. For wastewater treatment the organic matter with molecular weight more than 20 kDa effected significantly on the membrane pore density, and reducing factor a_2, whereas the membrane pore size reducing factor a_1 exhibited little or no relationship with organic matter with molecular weight less than 20 kDa.

Acknowledgments This work was supported by National Basic Research Program of China (973 Program, 2010CB732203), and National Natural Science Foundation of China (20374025). Dr. S. Liu thanks the goal-oriented project (SKLF-MB-200805) from State Key Laboratory of Jiangnan University.

References

Belfort G, Davis R, Zydney A (1994) The behavior of suspensions and macromolecular solutions in crossflow microfiltration. J Membr Sci 96:1–58

Bell C, Peppas N (1996) Water, solute and protein diffusion in physiologically responsive hydrogels of poly(methacrylic acid-g-rthylene glycol). Biomaterials 17:1203–1218

Burns D, Zydney A (1999) Effects of solution PH on protein transport through semipermeable ultrafiltration membranes. Biotechnol Bioeng 64:27–37

Burns D, Zydney A (2000) Buffer effects on the zeta potential of ultrafiltration membranes. J Membr Sci 172:39–48

Cai J, Zhang L, Chang C, Cheng G, Chen X, Chu B (2007a) Hydrogen-bond-induced inclusion complex in aqueous cellulose/LiOH/urea solution at low temperature. ChemPhysChem 8:1572–1579

Cai J, Wang L, Zhang L (2007b) Influence of coagulation temperature on pore size and properties of cellulose membranes prepared from NaOH–urea aqueous solution. Cellulose 14:205–215

Cai J, Zhang L, Liu S, Liu Y, Xu X, Chen X, Chu B, Guo X, Xu J, Cheng H, Han H, Kuga S (2008) Dynamic self-assembly induced rapid dissolution of cellulose at low temperatures. Macromolecules 41:9345–9351

Capar G, Yilmaz L, Yetis U (2006) Reclamation of acid dye bath wastewater: effect of pH on nanofiltration performance. J Membr Sci 281:560–569

Chan R, Chen V (2004) Characterization of protein fouling on membranes: opportunities and challenges. J Membr Sci 242:169–188

Clech P, Chen V, Fane T (2006) Fouling in membrane bioreactors used in wastewater treatment. J Membr Sci 284: 17–53

Cuissinat C, Navard P (2006) Swelling and dissolution of cellulose Part II: free floating cotton and wood fibres in NaOH-water-additives systems. Macromol Symp 244:19–30

Duclos-Orsello C, Li W, Ho C (2006) A three mechanism model to describe fouling of microfiltration membranes. J Membr Sci 280:856–866

Egal M, Budtova T, Navard P (2008) The dissolution of microcrystalline cellulose in sodium hydroxide-urea aqueous solutions. Cellulose 15:361–370

Fane A, Fell C (1987) A review of fouling and fouling control in ultrafiltration. Desalination 62:117–136

Gavillon R, Budtova T (2007) Kinetics of cellulose regeneration from cellulose-NaOH-water gels and comparison with cellulose-N-methylmorpholine-N-oxide-water solutions. Biomacromolecules 8:424–432

Hong S, Elimelech M (1997) Chemical and physical aspects of nom fouling of nanofiltration membranes. J Membr Sci 132:159–181

Isogai A, Usuda M, Koto T, Ulyu T, Atalla R (1989) Solid-state CP/MASS ^{13}C NMR study of cellulose polymorphs. Macromolecules 22:3168–3172

Kamide K, Iijima H, Matsuda S (1993) Thermodynamics of formation of porous polymeric membrane by phase separation method I: nucleation and growth of nuclei. Polym J 25:1113–1131

Khayet M, Khulbe K, Matsuura T (2004) Characterization of membranes for membrane distillation by atomic force microscopy and estimation of their water vapor transfer coefficients in vacuum membrane distillation process. J Membr Sci 238:199–211

Kim J, Yun S (2006) Discovery of cellulose as a smart material. Macromolecues 39:4202–4206

Liu S, Zhang L (2009) Effects of polymer concentration and coagulation temperature on the properties of regenerated cellulose films prepared from LiOH/urea solution. Cellulose 16:189–198

Loeb S, Sourirajan S (1963) Sea water demineralization by means of an osmotic membrane. Adv Chem Ser 38:117–132

Lue A, Zhang L, Ruan D (2007) Inclusion complex formation of cellulose in NaOH–thiourea aqueous system at low temperature. Macromol Chem Phys 208:2359–2366

Mao Y, Zhou J, Cai J, Zhang L (2006) Effects of coagulants on porous structure of membranes prepared from cellulose in NaOH/urea aqueous solution. J Membr Sci 279:246–255

Marshall A, Munro P, Tragardh G (1993) The effect of protein fouling in microfiltration and ultrafiltration on permeate flux, protein retention and selectivity: a literature review. Desalination 91:65–108

Mehta A, Zydney A (2006) Effects of membrane charge on flow and protein transport during ultrafiltration. Biotechnol Prog 22:484–492

Mosqueda-Jimenez D, Narbaitz R, Matsuura T (2004) Membrane fouling test: apparatus evaluation. J Environ Eng ASCE 130:90–98

Parameshwaran K, Fane A, Cho B, Kim K (2001) Analysis of microfiltration performance with constant flux processing of secondary effluent. Water Res 35:4349–4358

Pujar N, Zydney A (1994) Electrostatic and electrokinetic interactions during protein transport through narrow pore membranes. Ind Eng Chem Res 33:2473–2482

Qi H, Cai J, Zhang L, Nishiyama Y, Rattaz A (2008) Influence of finishing oil on structure and properties of multi-filament fibers from cellulose dope in NaOH/urea aqueous solution. Cellulose 15:81–89

Rabek J (1980) Experimental methods in polymer chemistry: applications of wide-angle X-ray diffraction (WAXD) to the study of the structure of polymers. Wiley Interscience, Chichester

Ruan D, Zhang L, Mao Y, Zeng M, Li X (2004a) Microporous films prepared from cellulose in NaOH/thiourea aqueous solution. J Membr Sci 241:265–274

Ruan D, Zhang L, Zhang Z, Xia X (2004b) Structure and properties of regenerated cellulose/tourmaline nanocrystal composite films. J Polym Sci Polym Phys 42:367–373

Samir M, Alloin F, Paillet M, Dufresne A (2004) Tangling effect in fibrillated cellulose reinforced nanocomposites. Macromolecules 37:4313–4316

Sang Y, Dong I, Younsook S, Hwan C, Hak Y, Yong S, Won H, Ji H (2005) Crystalline structure analysis of cellulose treated with sodium hydroxide and carbon dioxide by means of X-ray diffraction and FTIR spectroscopy. Carbohydr Res 340:2376–2391

Sescousse R, Budtova T (2009) Influence of processing parameters on regeneration kinetics and morphology of porous cellulose from cellulose–NaOH–water solutions. Cellulose 16:417–426

Singh S, Khulbe K, Matsuura T, Ramamurthy P (1998) Membrane characterization by solute transport and atomic force microscopy. J Membr Sci 142:111–127

Tao Y, Zhang L, Yan F, Wu X (2007) Chain conformation of water-insoluble hyperbranched polysaccharide from fungus. Biomacromolecules 8:2321–2328

Teixeira M, Rosa M, Nystrom M (2005) The role of membrane charge on nanofiltration performance. J Membr Sci 265: 160–166

Wang L, Wang X (2006) Study of membrane morphology by microscopic image analysis and membrane structure parameter model. J Membr Sci 283:109–115

Weng L, Zhang L, Ruan D, Shi L, Xu J (2004) Thermal gelation of cellulose in a NaOH/thiourea aqueous solution. Langmiur 20:2086–2093

Yang G, Zhang L (1996) Regenerated cellulose microporous membranes by mixing cellulose cuoxan with a water soluble polymer. J Membr Sci 114:149–155

Yuan W, Zydney A (1999) Effects of solution environment on humic acid fouling during microfiltration. Desalination 122:63–76

Zhao C, Zhou X, Yue Y (2000) Determination of pore size and pore size distribution on the surface of hollow-fiber filtration membrane: a review of methods. Desalination 129:107–123

Zhou J, Zhang L, Cai J, Shu H (2002) Cellulose microporous films prepared from NaOH/urea aqueous solution. J Membr Sci 210:77–90